Research Article | Vol. 6, No. 11 | 1 Nov 2016 | OPTICAL MATERIALS EXPRESS 3541

Optical Materials EXPRESS

Bandgap engineering of $Cu(In_{1-x}Ga_x)Se_2$ absorber layers fabricated using $CuInSe_2$ and $CuGaSe_2$ targets for one-step sputtering process

JAE-CHEOL PARK,[1] JEON-RYANG LEE,[1] MOWAFAK AL-JASSIM,[2] AND TAE-WON KIM[1,*]

[1]*Advanced Photoenergy Laboratory, Applied Optics and Energy Research Group, Korea Institute of Industrial Technology, Gwangju, 500-480, South Korea*
[2]*National Renewable Energy Laboratory, National Center for Photovoltaics, Golden, CO, USA*
[*]*twkim90@kitech.re.kr*

Abstract: We have demonstrated that the bandgap of $Cu(In_{1-x}Ga_x)Se_2$(CIGS) absorber layers was readily controlled by using a one-step sputtering process. CIGS thin-film sample libraries with different Ga/(In + Ga) ratios were synthesized on soda-lime glass at 550°C using a combinatorial magnetron sputtering system employing $CuInSe_2$(CIS) and $CuGaSe_2$(CGS) targets. Energy-dispersive X-ray fluorescence spectrometry (EDS-XRF) confirmed that the CIGS films had different Ga/(In + Ga) ratios, which were varied by the sample configuration on the substrate and ranged from 0.2 to 0.9. X-ray diffraction and Raman spectroscopy revealed that the CIGS films had a pure chalcopyrite phase without any secondary phase such as Cu-Se or ordered vacancy compound (OVC), respectively. Furthermore, we found that the optical bandgap energies of the CIGS films determined by transmittance measurements ranged from 1.07 eV to 1.53 eV as the Ga/(In + Ga) ratio increased from 0.2 to 0.9, demonstrating that the one-step sputtering process using CIS and CGS targets is another simple route to control the bandgap energy of the CIGS absorber layer.

OCIS codes: (350.6050) Solar energy; (040.5350) Photovoltaic; (160.4760) Optical properties.

References and links

1. M. G. Park, S. J. Ahn, J. H. Yun, J. Gwak, A. Cho, S. K. Ahn, K. Shin, D. Nam, H. Cheong, and K. Yoon, "Characteristics of Cu(In, Ga)Se_2 (CIGS) thin films deposited by a direct solution coating process," J. Alloys Compd. **513**, 68–74 (2012).
2. A. J. Han, Y. Zhang, W. Song, B. Li, W. Liu, and Y. Sun, "Structure, morphology and properties of thinned Cu(In,Ga)Se_2 films and solar cells," Semicond. Sci. Technol. **27**(3), 035022 (2012).
3. H. Zachmann, S. Heinker, A. Braun, A. V. Mudryi, V. F. Gremenok, A. V. Ivaniukovich, and M. V. Yakushev, "Characterization of Cu(In,Ga)Se_2-based thin film solar cells on polyimide," Thin Solid Films **517**(7), 2209–2212 (2009).
4. A. Hultqvist, C. Platzer-Bjorkman, J. Pettersson, T. Törndahl, and M. Edoff, "$CuGaSe_2$ solar cells using atomic layer deposited Zn(O,S) and (Zn,Mg)O buffer layers," Thin Solid Films **517**(7), 2305–2308 (2009).
5. L. Zhang, Q. He, W. L. Jiang, F.-F. Liu, C.-J. Li, and Y. Sun, "Effects of substrate temperature on the structural electrical properties of Cu(In,Ga)Se_2 thin films," Sol. Energy Mater. Sol. Cells **93**(1), 114–118 (2009).
6. D. G. Moon, S. J. Ahn, J. H. Yun, A. Cho, J. Gwak, S. K. Ahn, K. Shin, K. Yoon, H.-D. Lee, H. Pak, and S. Kwon, "Ex-situ and in-situ analyses on reation mechanism of $CuInSe_2$(CIS) formed by selenization of sputter deposited CuIn precursor with Se vaper," Sol. Energy Mater. Sol. Cells **95**(10), 2786–2794 (2011).
7. I. H. Choi, "Raman spectroscopy of $CuIn_{1-x}Ga_xSe_2$ for in-situ monitoring of the composition ration," Thin Solid Films **519**(13), 4390–4393 (2011).
8. N. H. Rafat and S. E.-D. Habib, "The limiting efficiency of band gap graded solar cells," Sol. Energy Mater. Sol. Cells **55**(4), 341–361 (1998).
9. T. Drobiazg, L. Arzel, A. Donmez, P. Zabierowski, and N. Barreau, "Influence of indium/gallium gradients on the Cu(In,Ga)Se_2 devices deposited by the co-evaporation without recrystallization," Thin Solid Films **582**, 47–50 (2015).
10. T. Klinkert, M. Jubault, F. Donsanti, D. Lincot, and J.-F. Guillemoles, "Differential in-depth characterization of co-evaporated Cu(In,Ga)Se_2 thin films for solar cell applications," Thin Solid Films **558**, 47–53 (2014).

#274782 http://dx.doi.org/10.1364/OME.6.003541
Journal © 2016 Received 29 Aug 2016; revised 6 Oct 2016; accepted 11 Oct 2016; published 17 Oct 2016

Optical Materials EXPRESS

11. G. S. Chen, J. C. Yang, Y. C. Chan, L. C. Yang, and W. Huang, "Another route to fabricate single-phase chalcogenides by post-selenization of Cu–In–Ga precursors sputter deposited from a single ternary target," Sol. Energy Mater. Sol. Cells **93**(8), 1351–1355 (2009).
12. S. U. Park, R. Sharma, and C. R. Lee, "A study on composition, structure and optical properties of copper-poor CIGS thin film deposited by sequential sputtering of CuGa/In and In/(CuGaþIn) precursors," J. Cryst. Growth **359**, 1–10 (2012).
13. Zs. Baji, Z. Labadi, G. Molnar, B. Pécz, A. L. Tóth, J. Tóth, A. Csik, and I. Bársony, "Post-selenization of stacked precursor layers for CIGS," Vacuum **92**, 44–51 (2013).
14. H. K. Song, S. G. Kim, and H. J. Joon, "Preparation of $CuIn_{1-x}Ga_xSe_2$ thin films by sputtering and selenization process," Sol. Energy Mater. Sol. Cells **75**(1-2), 145–153 (2003).
15. C. Y. Su, W. H. Ho, H. C. Lin, C.-Y. Nieh, and S.-C. Liang, "The effects of the morphology on the CIGS thin films prepared by CuInGa single precursor," Sol. Energy Mater. Sol. Cells **95**(1), 261–263 (2011).
16. S. J. Park and J. H. Kim, "Structural analysis of $Cu(In,Ga)Se_2$ films fabricated by using sputtering and post-selenization," Curr. Appl. Phys. **13**(6), 1046–1049 (2013).
17. K. Kushiya, M. Tachiyuki, T. Kase, I. Sugiyama, Y. Nagoya, D. Okumura, M. Sato, O. Yamase, and H. Takeshita, "Fabrication of graded band-gap $Cu(InGa)Se_2$ thin-film mini-modules with a $Zn(O,S,OH)_x$ buffer layer," Sol. Energy Mater. Sol. Cells **49**(1-4), 277–283 (1997).
18. Y. Nagoya, K. Kushiya, M. Tachiyuki, and O. Yamase, "Role of incorporated sulfur into the surface of $Cu(InGa)Se_2$ thin-film absorber," Sol. Energy Mater. Sol. Cells **67**(1-4), 247–253 (2001).
19. C. H. Chen, W. C. Shih, C. Y. Chien, C.-H. Hsu, Y.-H. Wu, and C.-H. Lai, "A promising sputtering route for one-step fabrication of chalcopyrite phase $Cu(In,Ga)Se_2$ absorbers without extra Se supply," Sol. Energy Mater. Sol. Cells **103**, 25–29 (2012).
20. J. A. Frantz, R. Y. Bekele, V. Q. Nguyen, J. S. Sanghera, A. Bruce, S. V. Frolov, M. Cyrus, and I. D. Aggarwal, "$Cu(In,Ga)Se_2$ thin films and devices sputtered from a single target without additional selenization," Thin Solid Films **519**(22), 7763–7765 (2011).
21. J. H. Shi, Z. Q. Li, D. W. Zhang, Q. Q. Liu, Z. Sun, and S. M. Huang, "Fabrication of $Cu(In, Ga)Se_2$ thin films by sputtering from a single quaternary chalcogenide target," Prog. Photovolt. Res. Appl. **19**(2), 160–164 (2011).
22. A. J. Zhou, D. Mei, X. G. Kong, X. H. Xu, L. D. Feng, X. Y. Dai, T. Gao, and J. Z. Li, "One-step synthesis of $Cu(In,Ga)Se_2$ absorber layers by magnetron sputtering from a single quaternary target," Thin Solid Films **520**(19), 6068–6074 (2012).
23. S. H. Jung, S. J. Ahn, J. H. Yun, J. Gwak, D. Kim, and K. Yoon, "Effects of Ga contents on properties of CIGS thin films and solar cells fabricated by co-evaporation technique," Curr. Appl. Phys. **10**(4), 990–996 (2010).
24. M. Steichen, J. Larsen, and P. J. Dale, "Preparation of $CuGaSe_2$ absorber layers for thin film solar cells by annealing of efficiently electrodeposited Cu–Ga precursor layers from ionic liquids," Thin Solid Films **519**(21), 7254–7258 (2011).
25. S. Roy, P. Guha, S. N. Kundu, H. Hanzawa, S. Chaudhuri, and A. K. Pal, "Characterization of $Cu(In,Ga)Se_2$ films by Raman scattering," Mater. Chem. Phys. **73**(1), 24–30 (2002).
26. H. Tanino, H. Deai, and H. Nakanishi, "Raman Spectra of CuGaxIn1-xSe2," Jpn. J. Appl. Phys. **32**(S3), 436–438 (1993).
27. S. K. Lee, J. K. Sim, and C. R. Lee, "Se interlayer in CIGS absorption layer for solar cell devices," J. Alloys Compd. **633**, 31–36 (2015).
28. S. Kang, R. Sharma, and C. R. Lee, "Band gap engineering of tandem structured CIGS compound absorption layer fabricated by sputtering and selenization," J. Alloys Compd. **563**, 207–215 (2013).
29. G. H. Bauer, S. Tardon, and S. Vignoli, "Quasi-Fermi level splitting and identification of recombination losses from room temperature luminescence in $Cu(In_{1-x}Ga_x)Se_2$ thin films versus optical band gap," Thin Solid Films **480–481**, 410–414 (2005).
30. K. Ramanathan, G. Teeter, and R. Noufi, "Properties of high-efficiency $CuInGaSe_2$ thin film solar cells," Thin Solid Films **480–481**, 499–502 (2005).
31. F. B. Dejene and V. Alberts, "Structural and optical properties of homogeneous $Cu(In,Ga)Se_2$ thin films prepared by thermal reaction of InSe/Cu/GaSe alloys with elemental Se vapour," J. Phys. D Appl. Phys. **38**(1), 22–25 (2005).
32. C. C. Chen, X. Qi, W. C. Chang, M.-G. Tsai, I.-G. Chen, C.-Y. Lin, P.-H. Wu, and K.-P. Chang, "The effects of pulse repetition rate on the structural, optical, and electrical properties of CIGS films grown by pulsed laser deposition," Appl. Surf. Sci. **351**, 772–778 (2015).
33. M. Saifullah, J. H. Moon, and J. H. Yun, "Effects of Cu content on the photovoltaic properties of wide bandgap CIGS thin-film solar cells prepared by single-stage process," Curr. Appl. Phys. **16**(11), 1517–1522 (2016).
34. H. X. Zhang and R. J. Hong, "CIGS absorbing layers prepared by RF magnetron sputtering from a single quaternary target," Ceram. Int. **42**(13), 14543–14547 (2016).

1. Introduction

$Cu(In_{1-x}Ga_x)Se_2$(CIGS) chalcopyrite compounds have been studied extensively for thin-film solar cells due to their high absorption coefficient (1×10^5 cm^{-1}) and controllable bandgap energy (1.04~1.67 eV) [1, 2, 32–34]. CIGS solar cells made by co-evaporation have shown

Optical Materials EXPRESS

record cell efficiencies exceeding ~20% in the laboratory scale [3–7]. To get such higher cell efficiency, the characteristics of CIGS absorber layers—including the structural, electrical, and optical properties—should be carefully optimized. Above all, bandgap engineering of CIGS absorber layers is very effective in improving cell performance, because the useful solar spectrum is determined by the absorption edge of the absorber layer. In addition, the technique of bandgap engineering can make bandgap grading in an absorber layer, which is necessary to get a higher efficiency by reducing the recombination losses and amplifying the carrier collection in the cell [8]. Indeed, co-evaporation is one of the preferred methods to control the bandgap of the CIGS absorber layer, demonstrating why the record efficiency was achieved using this method [9,10].

On the other hand, although the sputtering process has several advantages such as large-area deposition and high deposition rates, the precise control of the Ga/(In + Ga) ratio to engineer the bandgap of the CIGS absorber layer is relatively difficult [11–16]. In particular, bandgap engineering of CIGS absorber layers by the conventional sputtering process, which employs a post-selenization process, requires great sophistication to optimize the entire process [17,18]. Because bandgap engineering of the CIGS absorber layer is necessary for high conversion efficiency, a simpler and cost-effective process should be developed to adjust the Ga/(In + Ga) ratio to control the bandgap.

In this study, we suggest a one-step sputtering process in which $CuInSe_2$ (CIS) and $CuGaSe_2$ (CGS) targets are used to fabricate CIGS films with an adjusted bandgap. By using the one-step sputtering process, we can systematically and easily control the bandgap of the CIGS absorber layer, showing the method to be a relatively simple technique to create bandgap grading.

2. Experiment

The CIGS absorber layers were deposited on soda-lime glass (SLG) substrates using a combinatorial magnetron sputtering system employing CIS and CGS targets with a 1:1:2 stoichiometry, respectively. The targets employed had a 4-inch diameter and were purchased from High Purity Chemical Co. Japan. Deposition of CIGS absorber layers using one-step sputtering, in which CIGS absorber layers can be directly synthesized from compound chalcopyrite targets without an additional selenization process, has been well established as reported elsewhere [19–22]. In our case, CIGS absorber layers having a continuous gradient in Ga/(In + Ga) ratios have been deposited during a single batch. Using this technique, we made CIGS sample libraries having different Ga/(In + Ga) ratios on the SLG substrate, as shown in Fig. 1. The Ga/(In + Ga) ratio in the CIGS absorber layers were varied depending on the location on the substrate. In this study, bare SLG substrates instead of Mo-coated SLG were used for characterizing the bandgap directly from transmittance measurements. The deposition conditions previously optimized were as follows: substrate temperature, 550°C; ambient gas, Ar; gas flow rate, 30 sccm; process pressure, 0.43 Pa; RF power, 300 W; and distance from target to substrate, 150 mm. Five kinds of CIGS film samples with a size of 12 x 12 mm^2 have been deposited on the substrates with a size of 180 x 50 mm^2 using a patterned shadow mask.

The crystalline structures of CIGS absorber layers were examined by an X-ray diffractometer (XRD, Panalytical X'pert MPD). Surface morphology and cross-section images were analyzed by using a field-emission scanning electron microscope (FE-SEM, Quanta 200). Chemical compositions were determined by energy-dispersive X-ray fluorescence spectrometry (EDX-XRF, SHIMADZU). The phase analysis was performed by Raman spectroscopy having a He-Ne laser with 632-nm wavelength (JOVIN YVON SAS). Optical properties of films were measured using a UV-VIS-IR spectrometer (Varian Cary 5000).

Optical Materials EXPRESS

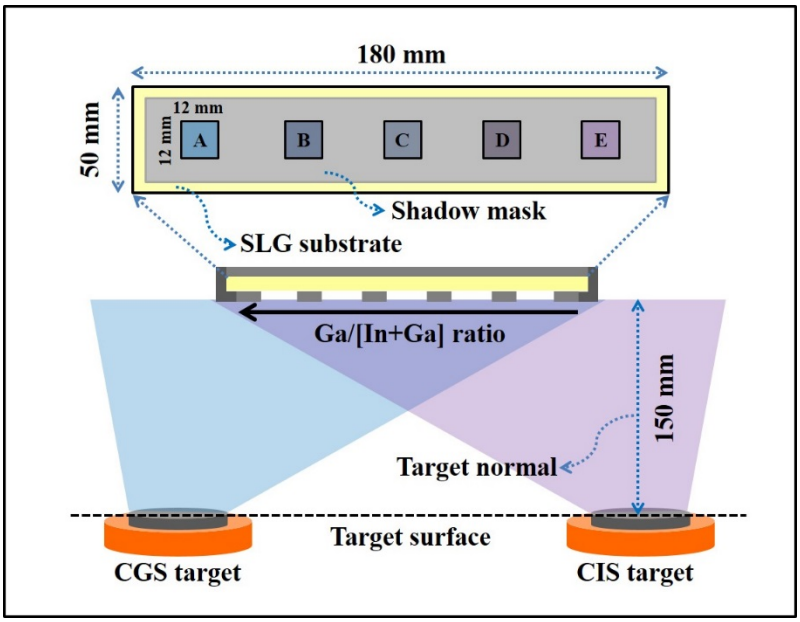

Fig. 1. Schematic diagram of a combinatorial magnetron sputtering system for growing CIGS thin films using CIS and CGS targets.

3. Results and discussion

3.1 Compositions

Table 1 shows the chemical composition of the CIGS samples determined by EDS-XRF, indicating that each sample has a significantly different Ga/(In + Ga) ratio while maintaining Cu/(In + Ga) and Se/(Cu + In + Ga) ratios. The Ga/(In + Ga) ratios of the samples are changed from 0.2~0.9 as a function of the location on the substrate. These results can be explained by the fact that the flux of sputtered particles from the each target have an angular dependence. Therefore, the CIGS sample libraries deposited on the SLG substrate have a continuous gradient in Ga/(In + Ga) ratios depending on the lateral distance from the target normal. These gradient in Ga/(In + Ga) ratios have been formed spontaneously under the configuration of the combinatorial sputtering system. Additionally, we have checked the ununiformity of the Ga/(In + Ga) ratios in each samples themselves by repeated measurements, however, the deviations of Ga/(In + Ga) ratios in each samples themselves were negligible.

Table 1. Chemical compositions of CIGS films determined by EDS-XRF.

Sample	Cu (at.%)	In (at.%)	Ga (at.%)	Se (at.%)	Ga / (In + Ga)	Cu / (In + Ga)	Se / (Cu + In + Ga)
A	27	3	20	50	0.9	1.2	1.0
B	27	5	17	52	0.8	1.2	1.1
C	27	7	14	52	0.7	1.3	1.1
D	27	10	11	52	0.5	1.3	1.1
E	25	19	5	51	0.2	1.1	1.0

3.2 SEM images

Figure 2(a) shows that the thickness of CIGS thin films range from 0.8 to 1.0 μm, which appear to be dense and have excellent adhesion to the SLG substrate for all samples. However, the surface morphology is remarkably different as a function of Ga/(In + Ga) ratio even though all the CIGS samples are deposited at the constant substrate temperature of

Optical Materials EXPRESS

550°C. Previously, we checked the surface morphologies of ternary thin films, which have the same growth conditions as the co-sputtered CIGS thin films, as shown in Fig. 2(b). The CGS thin films showed the densely packed grains without any void;but had small grains in the surface morphology. On the contrary, the CIS thin films showed the considerable improvement in grain sizes above 1μm scale. Despite the big differences in the morphological properties, no structural and optical changes was found in each film. The CIGS samples (A-D) co-deposited by using CIS and CGS targets, which have a Ga-rich characteristic, show a smoother surface and compact microstructure, whereas the CIGS sample (E) with Ga/(In + Ga) ratio of 0.2 exhibits irregular and facet-shaped structure. In regard to effects on Ga contents, it was reported that the CIGS thin films has smaller grains at the higher Ga content compared to the films grown at the low Ga content [23, 30]. This shows that the CIGS morphologies varied with Ga content in the CIGS thin films, showing that the CIGS samples (A-D) with high Ga content has the similar morphology like a CGS thin film.

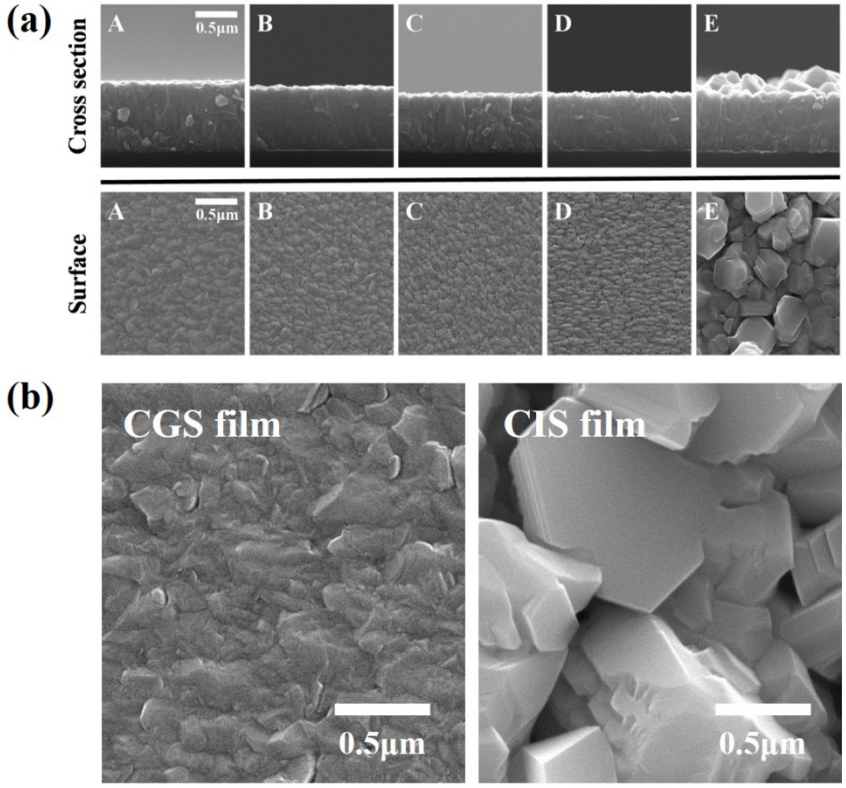

Fig. 2. (a). Cross-section and surface SEM images of CIGS thin films with different Ga/(In + Ga) ratios of (A) 0.9, (B) 0.8, (C) 0.7, (D) 0.5, and (E) 0.2, respectively, (b) surface images of CIS and CGS ternary thin films.

3.3 XRD patterns

The Fig. 3(a) shows the XRD patterns of CIGS thin films as a function of Ga/(In + Ga) ratio deposited at a substrate temperature of 550°C. All the CIGS thin films reveal dominant (112) peaks, including chalcopyrite characteristic peaks of (220), (204), and (312). Also, no secondary peaks indicating Cu-Se or OVC (ordered vacancy compound) phases are observed in the CIGS thin films despite using two different kinds of sputtering targets (CIS and CGS) at the same time. The slight peak split of CGS film is confirmed to be the distortion of lattice

Optical Materials EXPRESS

constant in the tetragonal CIGS structure due to high Ga content in CIGS thin films but not secondary phases [24]. In addition, the dominant (112) peaks are almost linearly shifted to high diffraction angle with increasing Ga/(In + Ga) ratio, as shown in Fig. 3(b). This is attributed to the decrease of the lattice parameter in the chalcopyrite CIGS structure by substituting In atoms with smaller Ga atoms. According to Scherrer equation ($\tau = K\lambda/\beta\cos\theta$), the crystallite size can be calculated by full-width at half-maximum (FWHM) values. The crystallite size of the CIGS thin films for (112) plane is ranged from 12 to 23nm and is slightly decreased at the Ga contents of 0.5 (sample D) and 0.7(sample C). This slight deviation can be explained by the fact that fluxes of particles are reduced at the center of substrate region. In other words, the main plasmas are located near the sputtering target normal, as mentioned in Fig. 1. The sample C and D were located at the place where fluxes of particles sputtered from both targets were the lowest due to the angular dependence of sputtering fluxes. For that reason, it is considered that the grain growth is slightly affected by the sputtered particles with low fluxes at the center of substrate region.

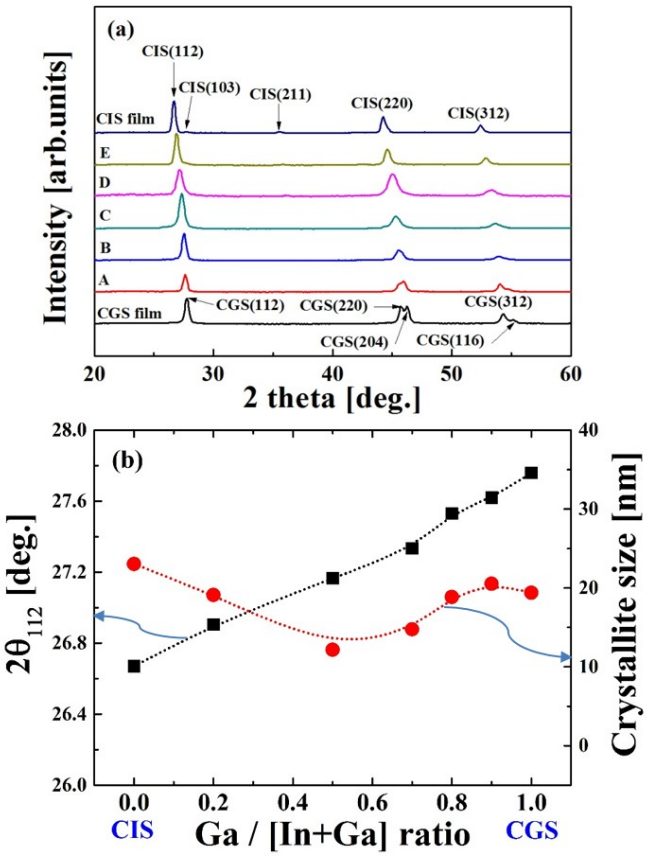

Fig. 3. XRD patterns (a) and crystallite size (b) of CIGS thin films as a function of Ga/(In + Ga) ratio.

3.4 Raman spectra

Raman spectroscopy was also used to check whether or not the CIGS thin films with different composition ratios of Ga/(In + Ga) are only chalcopyrite single phase. Generally, the frequency of the A1 mode in $Cu(In_{1-x}Ga_x)Se_2$ films shifts linearly from 173 cm^{-1} to 186 cm^{-1} with varying x from 0 to 1. According to the report of Roy et al. [25], the Raman shift caused

Optical Materials EXPRESS

by Ga content in CIGS thin films can be estimated by F = 173 + 12.92*x*, where F is the Raman shift value of A1 mode and *x* is the composition ratio of Ga/(In + Ga). This formula means that Raman frequency increases by substituting In sites with Ga atoms which have a lower mass than In atoms, resulting in a larger bond length formed in the lattice site [26]. In our case, we confirmed that the A1 mode frequency of CIGS films shifts from 173.4 cm^{-1} to 186.1 cm^{-1} with increasing Ga/(In + Ga) ratio from 0 to 1, as shown in Fig. 4(a), respectively. To confirm this relationship, composition ratio and A1 scattering peaks are depicted in Table 2. Raman shift values of A1 mode peaks are generally well matched with Ga/(In + Ga) ratios, but show a small deviation in sample B and C. Regarding the compositional behavior in physical property, accurate composition values should be accompanied but the Ga/(In + Ga) ratios determined by EDS-XRF measurements are not perfectly adjusted with above equation due to uncertainty of composition analysis, leading similar scattering peak positions in spite of different sample positions. However, it is clearly confirmed that A1 mode peak positions are systematically distributed as a function of Ga/(In + Ga) ratio, which is not fully consistent with composition ratio. In addition, the Fig, 4(b) shows that the FWHM values of all the CIGS thin films range from 9.2 to 12.5 cm^{-1}, demonstrating the high quality of CIGS thin films. Furthermore, B2 and E1 modes of the CIGS thin films are also observed, which correspond to the vibration mode of all CIGS atoms. Consequently, one-step sputtered CIGS thin films show only chalcopyrite characteristic peaks (A1, B2, E1 modes) regardless of Ga/(In + Ga) ratio in the CIGS films without any secondary phase.

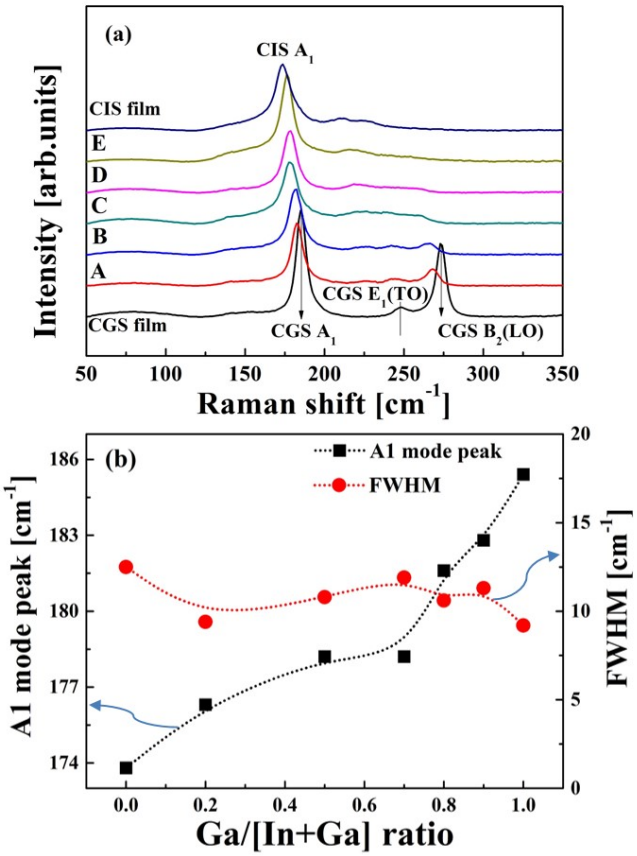

Fig. 4. Raman spectra of CIGS thin films (a) and those A1 scattering peaks and FWHM values (b) as a function of Ga/(In + Ga) ratio.

Optical Materials EXPRESS

Table 2. Raman shift values of CIGS thin films as a function of Ga/(In + Ga) ratio.

Sample	Composition ratio	A1 mode peaks (cm^{-1})	
	Ga / (In + Ga)	measured	calculated
CGS	1.0	186.1	185.9
A	0.9	183.1	184.6
B	0.8	181.7	183.3
C	0.7	178.4	182.0
D	0.5	178.4	179.5
E	0.2	176.3	175.6
CIS	0	173.4	173.0

3.5 Optical bandgaps

The optical bandgap energy (Eg) is studied by using transmittance, reflectance spectra from the CIGS absorber layer on a SLG substrate. The optical coefficient (α) can be deduced from the following equation [27]:

$$\alpha = \frac{1}{d} ln \left[\frac{\sqrt{(1-R)^4 + 4T^2R^2}}{2\mathrm{T}} + \frac{(1-R)^2}{2T} \right]$$

where d is the film thickness, T is the transmittance, and R is the reflectance. The CIGS compounds are direct transition semiconductors and the parabolic band diagram is given by the following equation [28]:

$$\alpha hv = A(hv - Eg)^{1/2}$$

where A is a constant that depends on the transition nature such as the effective mass and the refractive index, and v is the radiation frequency. By using the above equation, the optical bandgap can be determined by extrapolating the linear portion of $(\alpha hv)^2$ versus photon energy (hv). Figure 5 indicates the plot of $(\alpha hv)^2$ versus hv for CIGS thin films, and the inset shows the optical bandgap energies with different Ga/(In + Ga) ratios. Generally, the CIS and CGS thin films having stoichiometric composition exhibit the bandgap energy of 1.02 and 1.62 eV, respectively [29]. In our case, CIS and CGS films deposited at the substrate temperature of 550°C show the bandgaps of 0.98 and 1.62 eV, respectively. By using these stoichiometric single targets, we confirmed that the CIGS thin films exhibit the optical bandgaps of 1.07, 1.24, 1.35, 1.47, and 1.53 for the Ga content of 0.2, 0.5, 0.7, 0.8, and 0.9, respectively. In the previous study, it was reported that the bandgaps of ($CuIn_{1-x}Ga_xSe_2$) thin films grown by co-evaporation technique are followed by the relationship between x (Ga content) and $E_g(x) = 0.998 + 0.291x + 0.43x^2$ eV [31]. Figure 5(b) shows the variation of bandgaps as a function of Ga content in the reference (red circle) and co-sputtered CIGS thin films (black square), respectively. The optical bandgaps of co-sputtered CIGS thin films increase with the Ga content and have a good agreement with the expected bandgaps at each the Ga content. Nevertheless, a slight deviation in the bandgaps was observed as the Ga content exceeding 0.7, which can be caused by the inaccuracy in the determination of compositions between the two studies. However, it should be noted that the bandgaps correspond approximately with the Ga content in the CIGS thin films, which have sharp absorption edges with fewer defects and good crystallinity for all the samples.

Optical Materials EXPRESS

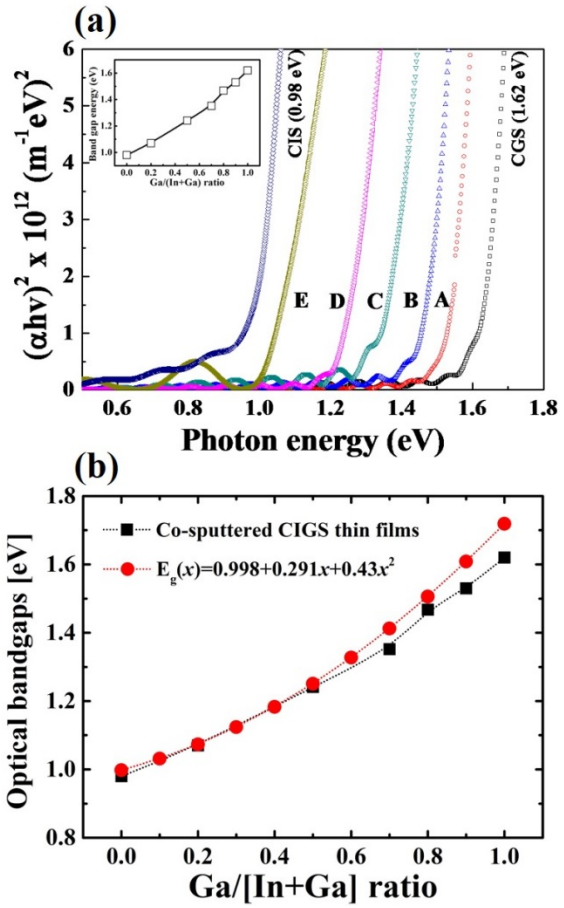

Fig. 5. (a) Plots of (hv)2 versus hv for co-sputtered CIGS thin films as a function of Ga content and (b) variation in the bandgaps with different Ga contents (black square : co-sputtered CIGS thin films, red circle : Ref. [31]).

4. Conclusion

In summary, we have introduced a systematic approach to obtain CIGS films with different (In,Ga) ratios by one-step sputtering without a selenization process using a combinatorial magnetron sputtering system from a CIS/CGS stoichiometric single target. The CIGS thin films show that the composition ratio of Ga/(In + Ga) consistently changed from 0.2 to 0.9 depending on the distance from the substrate to each sputtering target (CIS and CGS). XRD patterns reveal that diffraction peak positions are linearly shifted to high angle for both (112) and (220) planes with increasing Ga/(In + Ga) ratio. Raman spectra also exhibit similar properties to the XRD patterns, demonstrating high-quality CIGS thin films with A1 mode scattering peak in each composition ratio. Moreover, the optical property shows that bandgap energies are also consistent with the composition ratio of Ga/(In + Ga), while maintaining the standard bandgap energy.

Funding

Korea Institute of Industrial Technology (KITECH) (EO160024); National Renewable Energy Laboratory (NREL) (DE-AC36-08GO28308).